J Mater Sci (2007) 42:4197–4204
DOI 10.1007/s10853-006-0642-2

The influence of magnetron sputtered silver and titanium coatings on the compaction and properties of surface modified PM Ti-48Al powders

Filipe Neves · Nelson Duarte · Bruno Trindade

Received: 16 January 2006 / Accepted: 5 July 2006 / Published online: 2 March 2007

Abstract Thin layers of silver and titanium were deposited onto commercial Ti–$_{48}$Al particles by magnetron sputtering prior to their consolidation by hot isostatic pressing and subsequent heat treatment. Based on picnometry and electron probe microanalysis results, average values of 1.5 and 2.5 at.%, respectively, were obtained for the silver and titanium contents in the coated particles. The surface modified Ti–$_{48}$Al particles exhibited improved sintering ability than the unmodified ones. The consolidated samples have duplex microstructures formed by γ-TiAl and γ-TiAl + α_2-Ti_3Al grains. Ag-rich nanoprecipitates were detected in the microstructure of the compacted Ti-$_{48}$Al + Ag sample. The coatings are no longer visible at the grains boundaries after a subsequent homogenization heat treatment at 1200°C. The highest values of hardness and Young's modulus were obtained for the Ti–$_{48}$Al + Ag sample, associated with a higher density and a lower percentage of pores.

Introduction

Both ingot and powder metallurgy techniques have been used to synthesize TiAl-based intermetallic alloys [1]. The low density, high melting point, and good elevated-temperature mechanical properties make these materials suitable for applications in the gas turbine and automotive industry. However, material processing and alloy development with the aim of improving low-temperature ductility of γ-TiAl based alloys, while retaining their strength at elevated temperatures, have become the major challenges in the last decades.

Many far from equilibrium processing techniques (e.g. mechanical alloying) have long been used as primary synthesis techniques to produce mixtures with intermetallic compositions from elemental alloy powders. TiAl intermetallics formed by metastable phases, such as supersaturated solid solutions, nanocrystalline and amorphous alloys [2] have been obtained with improved mechanical properties [3]. However, their consolidation process is one of the crucial steps in obtaining high performance components. The temperature required for a good hot compaction of intermetallic mixtures (e.g., Hot Isostatic Pressing) is relatively high, mainly due to the high melting points of the ordered structures. One of the ways to overcome this problem is to use composite powders. The development of composite powders usually implies a combination of two or more components, which must be pressed and sintered. Moreover, they must be as homogeneous as possible in order to produce suitable final products.

Different methods have been applied in the industry for producing composite powders, such as mixing (blenders, mills), evaporation of a liquid containing a soluble metal salt, chemical vapor deposition and the use of an organic powder binder before the sintering treatment, among others. In a

F. Neves
INETI, DMTP, Estrada do Paço do Lumiar no 22,
1649-038 Lisboa, Portugal

N. Duarte · B. Trindade (✉)
Mechanical Department – Polo II of the Coimbra University, University of Coimbra, Pinhal de Marrocos, Coimbra 3030-788, Portugal
e-mail: bruno.trindade@dem.uc.pt

recent paper [4], we described a new procedure for the synthesis of intermetallic–matrix composites (IMC) from powders coated by magnetron sputtering and consolidated by hot isostatic pressing (HIP). This procedure has been applied to the production of Ti_5Si_3 intermetallic compacts from mechanically alloyed mixtures coated with aluminum and titanium. A good choice of coating is crucial to increase the performance of the final component by the formation of a second phase at the interface of the particles. Moreover, depending on its melting point, it might even decrease the temperature of the consolidation process.

In this study, thin layers of silver and titanium were deposited onto commercial Ti–$_{48}$Al particles by magnetron sputtering prior to their consolidation by HIP and subsequent heat treatment with the aim of improving the sintering ability and the mechanical properties of the hot isostatically pressed compacts.

Experimental details

Commercial Ti–$_{48}$Al powders with a maximum particle size of 75 μm were coated with Ag and Ti by d.c magnetron sputtering with a specific discharge power of 2.62×10^{-2} W/mm^2, for 60 min and 90 min, respectively. The depositions were performed in a pure argon atmosphere (0.5 Pa) after chamber evacuation down to a base pressure of 10^{-4} Pa. During the depositions the powders were continually shaken by vibration and translation movements in order to obtain homogeneous coatings.

The powders with and without Ag- or Ti-coating were firstly consolidated by cold isostatic pressing at 250 MPa and 350 MPa, respectively, and later by hot isostatic pressing at 900 °C/150 MPa/2 h, as described elsewhere [4]. Finally, the compacts were heat treated at 1200°C for 4 h in vacuum to homogenize the microstructure.

Before the metallographic observations, the cylindrical bars were cut and polished with diamond down to 3 μm, and finally etched with a modified Kroll etching solution. The phase constituents of the samples were analyzed by means of X-ray diffraction (XRD) using an X'pert Philips equipment with Cu-K_α radiation. The thermal behavior of the coated and uncoated samples was evaluated by Differential Thermal Analysis (DTA), in a Labsys TG/DTA Setaram equipment, applying a heating rate of 0.25 K/s. A Philips XL30 FEG Scanning Electron Microscope (SEM) equipped with Energy-Dispersive X-ray Spectroscopy (EDS) from EDAX was used for the surfaces analysis. Electron Probe Microanalysis (EPMA)—Camebax SX50 from CAMECA—was also used for chemical analysis.

Particle size distributions were determined by laser scattering (Cilas 1064 equipment) from a powder suspension in water under mechanical agitation after a 60-s sonication. Sample density was measured by He Picnometry (Micromeritics Accupy 1330). Porosity of the samples was evaluated by mercury porosimetry (Micromeritics 9320).

Microhardness measurements were carried out on flat polished surfaces using a Vickers diamond indenter for determination of the hardness and Young's modulus of the compacts, according to the method described in [5]. In this method, the indentation modulus, E_r, can be obtained according to the equation:

$$E_r = \frac{1}{2}\left(\frac{\pi}{A_c}\right)^{\frac{1}{2}} \frac{1}{C - C_o} \tag{1}$$

where A_c is contact area of the indentation immediately before unloading, $C = dh/dp$ is the total compliance of the system, i.e. the inverse of the slope of the load (P)—penetration depth (h) curve at the beginning of the unloading and C_o is the frame compliance. The indentation modulus, E_r, is a function of the Young's modulus, E, and the Poisson ratio, υ, of the specimen and the indenter through:

$$\frac{1}{E_r} = \frac{(1 - \upsilon_s^2)}{E_s} + \frac{(1 - \upsilon_i^2)}{E_i} \tag{2}$$

where the subscripts s and i indicate the specimen and indenter, respectively. A 0.5 N load was used in this work for the determination of the hardness and Young's modulus values of the compacts.

Results

The commercial Ti–$_{48}$Al powders have a unimodal particle size distribution (Fig. 1a), with d_{50} = 49.3 μm, and they are composed mainly of γ-TiAl phase (Fig. 1b) with the α-Ti_3Al as minor phase. One of the Ti–$_{48}$Al particles was mechanically polished and its chemical composition determined along a straight line (Fig. 2). The results show a chemical composition gradient characterized by regions close to the surface richer in Al. Moreover, all the performed measurements reveal an alloy slightly richer in Al than expected. An average chemical composition of Ti–$_{50.3}$Al (at.%) was obtained for the powders from 50 measurements performed in different particles (10 measurements in each particle). According to the

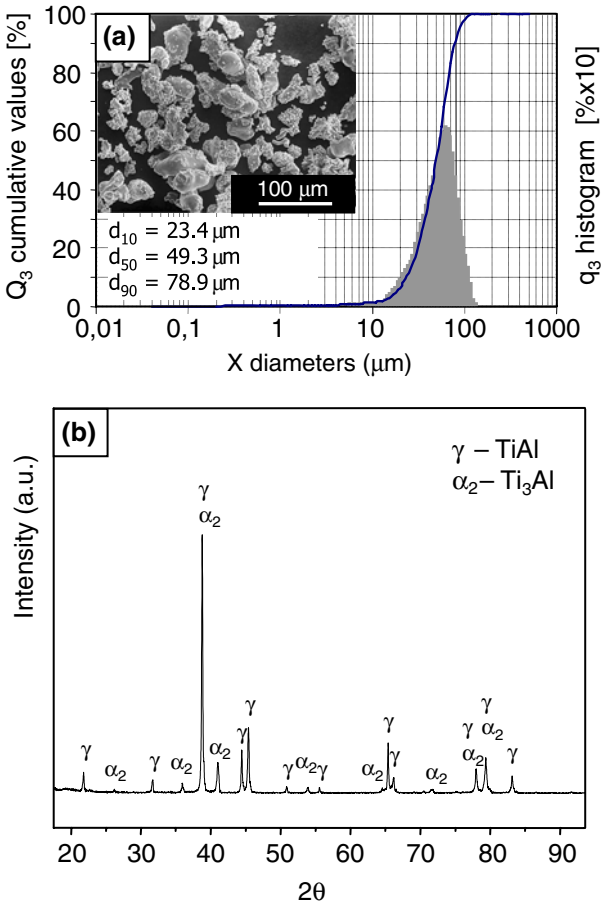

Fig. 1 (**a**) Particle size distribution and (**b**) X-ray diffraction pattern of Ti–$_{48}$Al powders

supplier, these powders are obtained by sintering a blend of powders of Al and Ti in order to achieve alloying by diffusion. Based on the results one might say that the process used for the production of the Ti–$_{48}$Al powders did not lead to chemically homogeneous powders.

After sputtering deposition the particle size distributions of the Ag- and Ti-coated particles were determined and compared with the one of the uncoated particles (Table 1). As can be seen, an increase of the d_{50} value was obtained in both cases,

Table 1 Particle size distributions of coated and uncoated Ti–$_{48}$Al powders

	Ti–$_{48}$Al	Ti–$_{48}$Al + Ag	Ti–$_{48}$Al + Ti
d_{10} (μm)	23.4	26.1	25.7
d_{50} (μm)	49.3	51.9	51.4
d_{90} (μm)	78.9	79.6	77.8

the increase being more significant in the case of the Ag-coating. This can be explained by the different sputtering yield rates of the elements Ag and Ti, which lead to different thicknesses of the coatings. According to the literature [6] the sputtering yield rates of Ag and Ti elements are 3.1 and 0.5 atoms/ion, respectively, for argon ions at 500 eV and 1 mA/cm^2 beam current density.

The density of the coated materials was evaluated by He picnometry (real density—ρ_R) and through the determination of the mass/volume ratio (volumetric density—ρ_V) of green samples compacted by cold isostatic pressure (CIP). The applied pressure varied in accordance with the chemical composition of each mixture. In the case of the uncoated powders a pressure of 350 MPa was necessary in order to obtain consistent green samples whereas for the coated powders a pressure of 250 MPa was sufficient. Table 2 shows the values obtained for the density and the weight percentage of the coating element determined by converting the volume percentages given by the following equation:

$$f \times \rho_{R(i)} + (1 - f) \times \rho_{R(c)} = \rho_{R(f)} \quad (3)$$

in which f and $(1–f)$ are the volume fractions of the uncoated particles and the coating element (Ag or Ti), respectively, $\rho_{R(i)}$ is the initial density of the uncoated Ti–$_{48}$Al, $\rho_{R(c)}$ is the density of the coating element and $\rho_{R(f)}$ is the final density of the coated Ti–$_{48}$Al particles. Therefore, equation (3) concerns the increase of the particle density provoked by the presence of the coating. Values of 10.49 g/cm^3 and 4.51 g/cm^3 [7] were used for the densities of the Ag and Ti coatings,

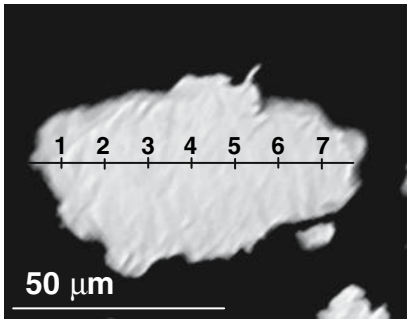

Point	Al (at.%)	Ti (at.%)
1	53.4	46.6
2	49.8	50.2
3	50.0	50.0
4	50.8	49.2
5	50.4	49.6
6	52.3	47.7
7	54.7	45.3

Fig. 2 Ti–$_{48}$Al commercial particle and chemical composition results (at.%) along a straight line

Table 2 Density of the green compacts and estimated % of the coating elements (Ag and Ti) in the samples

	Mass and dimensions after CIP			Density (g/cm^3)			Estimated % of the coating element wt.% (at.%)
	Mass(g)	Dia. (cm)	h (cm)	m/v (ρ_v)	Pic. He (ρ_R)	$\rho_v/\rho_{R\ (\%)}$	
Ti–$_{48}$Al	6.31	1.05	2.62	2.76	3.86	72	–
Ti–$_{48}$Al + Ag	5.40	1.03	2.31	2.81	4.05	69	7.0 (2.5)
Ti–$_{48}$Al + Ti	6.20	1.09	2.48	2.70	3.88	69	1.8 (1.4)

respectively. By solving this equation, estimated percentages of 7.0 wt.% (2.5 at.%) and 1.8 wt.% (1.4 at.%) were obtained for silver and titanium contents, respectively. These values are consistent with the ones obtained by EPMA in different zones of the samples (analysis in 1×1 mm^2 area). Average values of 2.4 ± 0.2 at.% Ag and 51.3 ± 0.1% Ti were obtained for the Ti–$_{48}$Al + Ag and Ti–$_{48}$Al + Ti samples, respectively. Therefore, considering the initial chemical composition of the powders measured by EPMA (Ti/Al = 0.99), one might say that the Ti coating contributes with about 1.5 at.% for the overall composition of the Ti–$_{48}$Al + Ti sample.

Figure 3 shows a SEM-BE image (Fig. 3a) and the Ag elemental distribution (Fig. 3b) of the Ti–$_{48}$Al + Ag particles. The Ag coating is reasonably uniform with an average thickness of 1 μm. With respect to the Ti-coating, a quantitative chemical analysis along a line crossing two particles is shown in Fig. 4. As expected, an increase in the Ti (K_α) signal (and a correspondent Al (K_α) signal decrease) is observed at the boundary of the two particles as a result of the presence of the Ti-coating. The reason that the aluminum percentage value is not zero at the interface of the two particles can be explained by the thickness of the coating (which is thinner than the Ag coating) and consequently by the inevitable contributions of the adjacent areas to the measured x-ray signal.

XRD analysis performed in the cross section of the green compacts (Fig. 5) confirms the presence of the fcc-Ag in the coated Ti–$_{48}$Al particles. However, no peaks ascribed to one or both the α- or β-Ti were detected in the XRD pattern of the Ti-coated sample, which may be related to the thin (<0.5 micron in Fig. 4) Ti coating.

All the Ti–$_{48}$Al samples with and without coating were consolidated by HIP. The main objective was the production of chemically homogenous materials with low porosity. The temperature and the time are two critical parameters in the HIP consolidation process since they play an important role not only in the final grain size but also in the density of the compacts. According to some authors, γ-TiAl powder of conventional grain size can only be consolidated to full density by HIP at temperatures equal or higher than 1,100 °C [8]. However, for mixtures obtained by far from equilibrium techniques, it seems that the small crystallite size enables superplastic deformation at ≈800 °C [9]. In the present work a relatively low HIP temperature was used (900 °C) to consolidate commercial Ti–$_{48}$Al powders with and without surface modification. The aim was to study the influence of the coatings on the quality of the final compacts, i.e., relative density (porosity). Nevertheless, before HIP the samples were submitted to DTA runs up to 900 °C with the aim of studying the phase transformations that would occur during HIP.

The DTA results showed no significant peaks in the heating curves of the Ti–$_{48}$Al and Ti–$_{48}$Al + Ti samples. On the contrary, a small endothermic peak was detected near 820 °C for the Ag containing sample. Taking into account that the melting point of silver is 962 °C, it is likely that the observed peak is associated with a eutectic transformation (γ-TiAl + Ag → L), as

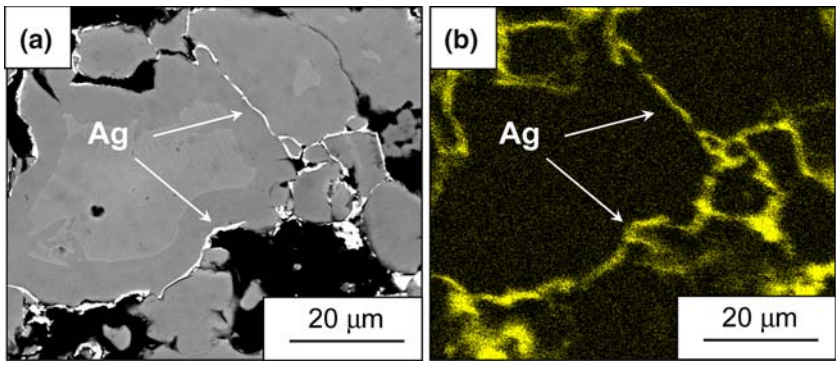

Fig. 3 (**a**) SEM-BE image of the Ti–$_{48}$Al particles coated with Ag and (**b**) elemental distribution of Ag in the particles (Ag L_α)

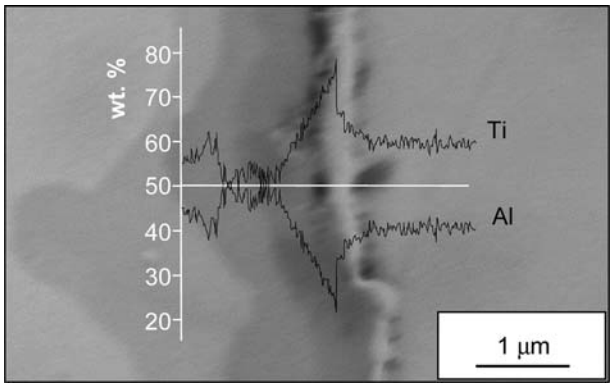

Fig. 4 Ti (K_α) and Al (K_α) signals across two particles

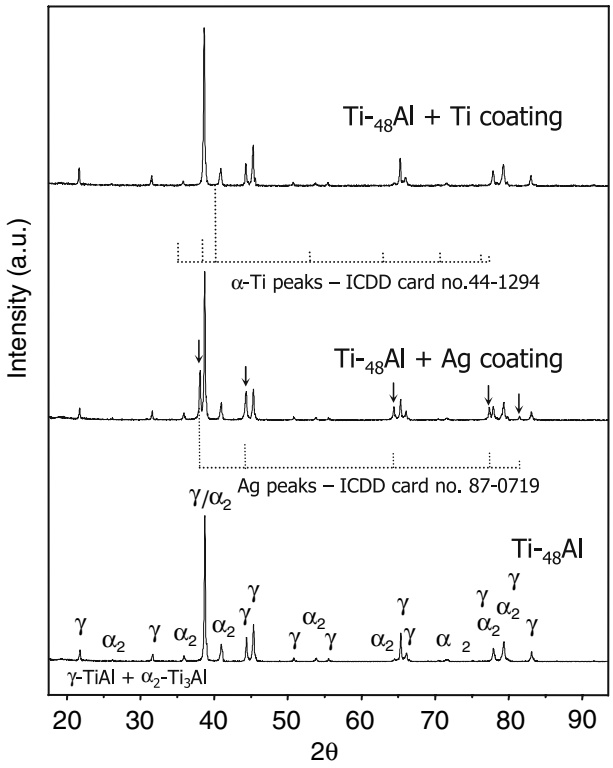

Fig. 5 XRD patterns of the $Ti_{-48}Al$ powders with and without Ag and Ti coatings

stated by Hashimoto et al. [10]. Hence, the compaction of the $Ti_{-48}Al$ + Ag sample at 900 °C will occur in the presence of a liquid phase containing Ag.

Figure 6 shows scanning electron micrographs of the etched HIPed samples. Their microstructures reveal some pores with a micrometer size, especially for the uncoated and Ti-coated samples. The percentage of open pores was calculated by mercury porosimetry. Values of 5%, 0.9% and 3% were obtained for the $Ti_{-48}Al$, $Ti_{-48}Al$ + Ag and $Ti_{-48}Al$ + Ti samples, respectively, which are consistent with the SEM observations. Therefore, the deposition of a Ti or Ag thin layer on $Ti_{-48}Al$ commercial particles increases their sintering ability, leading to a decrease of porosity. This is particularly true for the Ag coated sample. Ag is a ductile fcc metal which permits high deformation at the surface of the particles, increasing their sintering behavior and consequently the densification of the sample. The existence of a relatively high percentage of pores in the $Ti_{-48}Al$ uncoated sample is not a surprising result since, as already mentioned, γ-TiAl powder of conventional grain size can only be consolidated to full density by HIP at higher temperatures ($T \geq 1{,}100$ °C).

The microstructure of the compacts is not homogeneous. In general, the grains exhibit a central region of a lighter shade surrounding by a darker region in backscattered electron images. EDS analysis showed the composition of the core to be close to the α_2 phase and the surrounding areas to the γ phase. Moreover, in some particles, the existence of a lamellar γ-TiAl + α_2-Ti_3Al structure is perceptible, in particular for the Ti-coated sample (Fig. 6c). High magnification SEM observations of these samples showed details of the microstructure. Both samples are formed by grains with different microstructure and chemical composition, corresponding mainly to the γ and $\gamma + \alpha_2$ phases. Precipitates with a nanometric size (<50 nm) were detected in the Ag-coated sample, near grain boundaries, dispersed in the γ matrix. EPMA results obtained from different regions of the samples are consistent with the SEM observations. Chemical compositions of $Ti_{-46}Al_{-4}Ag$ and $Ti_{-40}Al$ were obtained for the γ and $\gamma + \alpha_2$ grains, respectively. In addition, measurements performed on the nanoprecipitates, showed that, as expected, these are Ag-rich. However, it was not possible to ascribe their formation to an established phase due to their very small size, which also did not allow the unequivocal determination of their chemical composition.

A decrease of the Ag- and Ti-coatings thickness was observed after HIP (500 nm and 250 nm, respectively). This means that these elements diffused from the interface into the grains during hot compaction. This result is corroborated by XRD analysis (Fig.7). Contrarily to the XRD pattern of the coated powders, the (111) peak of the fcc-Ag phase is hardly detected in the XRD pattern of the HIPed sample. Since HIP did not lead to important chemical composition variations, one might say that only a small portion of this element (the one allocated in the particle boundaries) contributed for diffraction. The small size of the Ag-rich precipitates is responsible for the absence of well-defined diffraction lines in the XRD pattern.

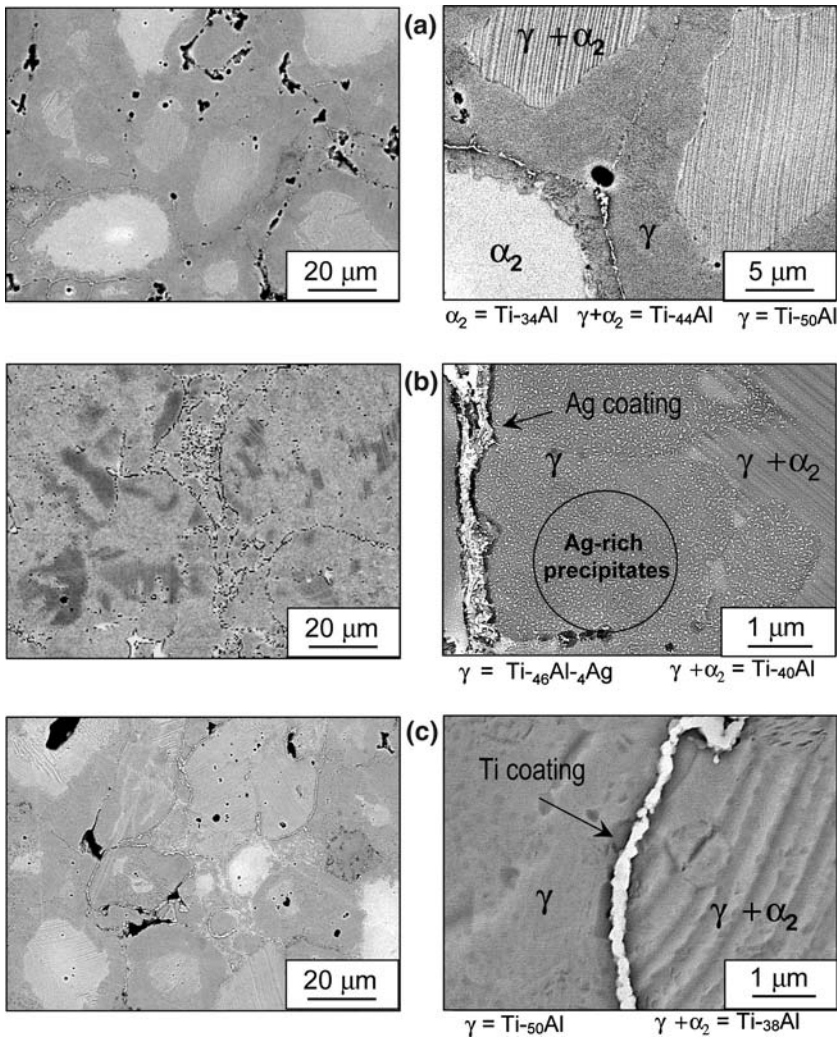

Fig. 6 SEM-BE images of the HIPed samples (900 °C/ 150 MPa/ 2 h). (**a**) $Ti_{-48}Al$, (**b**) $Ti_{-48}Al$ + Ag and (**c**) $Ti_{-48}Al$ + Ti

Table 3 compares the hardness values of the HIPed compacts, and it shows that the hardness of the $Ti_{-48}Al$ + X (X = Ag, Ti) samples is lower than that of the uncoated sample, as a result of the presence of a softer phase at the particles' surface. The values obtained varied from 2.9 GPa ($Ti_{-48}Al$ + Ag sample) to 3.5 GPa ($Ti_{-48}Al$ sample) and are comparable with the ones reported in the literature for (Ti-Al)-based materials consisting of $\gamma + \alpha_2$ phases [11]. The existence of a softer phase in the particle boundaries is responsible for the hardness decrease, which is particularly true for the $Ti_{-48}Al$ + Ag sample. An even lower hardness value for this sample might be expected if the fine precipitation in the γ-matrix did not occur.

After HIP, the samples were vacuum heat treated at 1,200 °C for 4 h in order to obtain stabilized microstructures. The heat-treatment did not lead to major microstructural changes. However, the coatings were no longer visible at the grains boundaries (Fig. 8). This implies that Ti and probably some Ag diffused into the matrix during this annealing treatment. The Ag-rich nanoprecipitates are evident throughout the microstructure. This explains the absence of the fcc-Ag reflections in the XRD pattern of the heat-treated $Ti_{-48}Al$ + Ag sample (Fig. 9) and would support the study of F. Neves et al. [12] which reports a solubility of about 2.5 at.% Ag in the γ-phase. However, the results obtained in the present study point towards an insignificant role of this element in the *c*/*a* ratio of the γ-phase as a consequence of the similarity of the atomic radii of elements Ti, Al and Ag (1.47, 1.43 and 1.44 Å [13]). Indeed, *c*/*a* values of 1.021 and 1.019 were obtained for the uncoated and Ag-coated samples, respectively. Apart from this, the heat treatment did not induce any structural transformation, the γ-TiAl and α_2-Ti_3Al phases coexisted in all samples after heating up to 1,200 °C.

The density and porosity of the annealed samples were also evaluated (Table 4). Regarding porosity, the values obtained are slightly lower than the ones

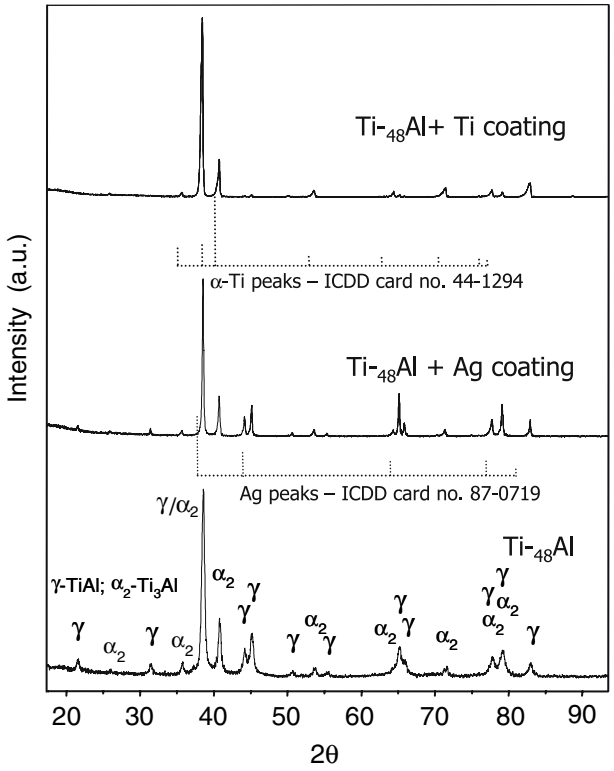

Fig. 7 XRD patterns of the samples HIPed at 900 °C/ 150 MPa/ 2 h

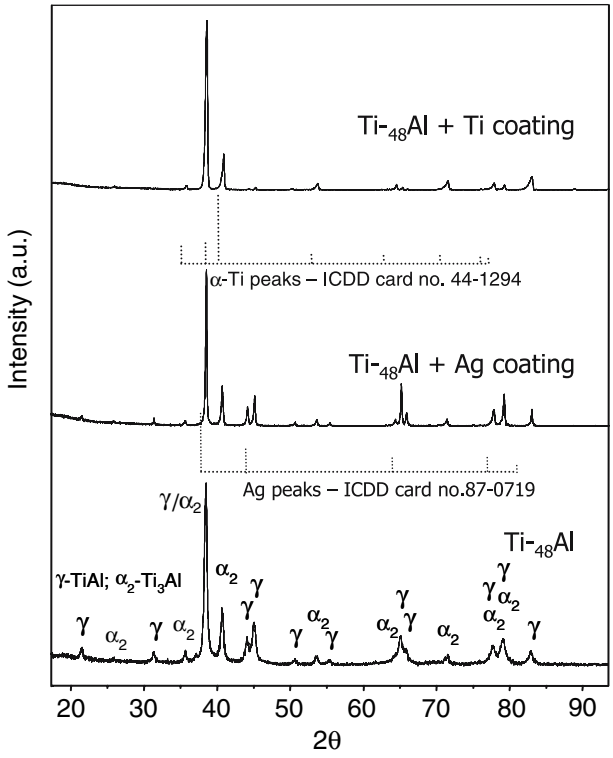

Fig. 9 XRD patterns of the heat-treated samples (1,200 °C/4 h)

Table 3 Hardness (H) of the HIPed samples

	$Ti_{-48}Al$	$Ti_{-48}Al$ + Ag	$Ti_{-48}Al$ + Ti
H (GPa)	3.5 ± 0.1	2.9 ± 0.2	3.1 ± 0.1

Table 4 Density and porosity of the annealed samples

	$Ti_{-48}Al$	$Ti_{-48}Al$ + Ag	$Ti_{-48}Al$ + Ti
ρ (g/cm^3)	3.85 ± 0.01	4.00 ± 0.02	3.78 ± 0.01
Porosity (%)	3.2	0.8	2.8

obtained for the HIPed samples. This suggests that annealing was useful for the densification of the samples. Consequently, no temperature induced porosity (TIP) was observed in this study in opposition to the observations of Wegmann et al. [14] in compacts obtained by HIP from powders atomized in inert gas atmospheres. This is a consequence of the powders we used, which, as stated before, were produced by sintering a blend of powders of Al and Ti without resource of an inert gas (e.g., Argon) as an atomization medium. It should be noted that according to Wegmann et al. [14] the gas is entrapped during atomization and probably stored in micro-pores, which grow substantially by during high temperature exposure.

The mechanical properties of the heat-treated samples are listed in Table 5. The hardness (H) and Youngs modulus (E) of the samples varied within the ranges 2.8–3.6 GPa, and 169–191 GPa, respectively.

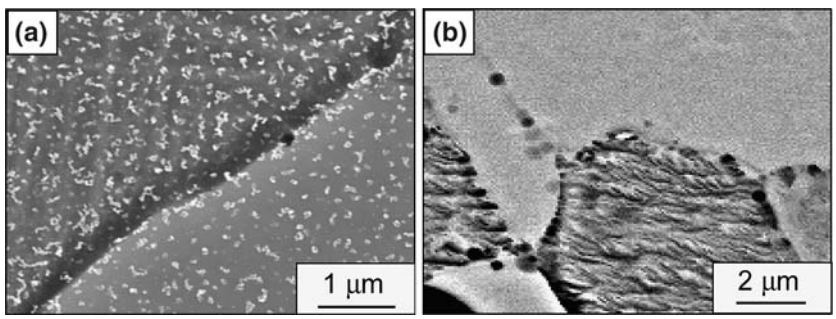

Fig. 8 (**a**) SEM-BE images of the heat treated samples (1,200 °C /4 h). (**a**) $Ti_{-48}Al$ + Ag and (**b**) $Ti_{-48}Al$ + Ti

Table 5 Hardness and Young's modulus of the annealed samples

	$Ti–_{48}Al$	$Ti–_{48}Al$ + Ag	$Ti–_{48}Al$ + Ti
H (GPa)	2.8 ± 0.1	3.0 ± 0.1	3.6 ± 0.05
E (GPa)	169 ± 5	191 ± 5	178 ± 6

These results are consistent with the values reported in the literature for (Ti–Al)-based materials consisting of γ and α_2 phases [11, 15].

In contrast to the $Ti–_{48}Al$ sample, the hardness of the coated samples increased during heat treatment. With regard to the compact containing Ag, it is likely that the slight hardness improvement be associated with the formation of the aforementioned nanoprecipitates. However, for the $Ti–_{48}Al$ + Ti sample the hardness increase might be explained by the incorporation of a certain amount of contaminant elements (oxygen and/or nitrogen), which produce some hardening. This phenomenon has already been observed in another study concerning the surface modification of $Ti_x–Si_{100-x}$ (x = 62.5 and 85 at.%) powders by the sputtering deposition of Ti thin layers [4] in which a relatively high oxygen content was detected in the particle boundaries of the compacts.

Conclusions

Magnetron sputtering was used for surface modification of $Ti–_{48}Al$ commercial powders. Based on picnometry and electron probe microanalysis results, average values of 2.5 and 1.5 at.%, respectively, were obtained for the silver and titanium contents in the coated particles. The surface modified $Ti–_{48}Al$ particles exhibited a higher densification ability than the unmodified ones. The HIPed and heat-treated samples were characterized by duplex microstructures consisting of γ-TiAl and γ-TiAl + α_2-Ti_3Al grains. Ag-rich nanoprecipitates were detected in the microstructure of the $Ti–_{48}Al$ + Ag sample. This material had the highest values of hardness and Youngs modulus, and was associated with a higher density and a lower percentage of pores compared to the other materials tested.

Acknowledgements The authors gratefully acknowledge the financial support from Portuguese Foundation for Science and Technology (FCT) through project POCTI/CTM/46498/2002.

References

1. Thomas M, Raviart JL, Popoff F (2005) Intermetallics 13(9):944
2. Oehring M, Yan ZH, Klassen T, Bormann R (1992) Phys Stat Sol A 131:671
3. Koch CC (1998) Mater Sci Eng A 244:39
4. Simões F, Trindade B (2005) Mater Sci Eng A 397:257
5. Antunes JM, Cavaleiro A, Menezes LF, Simões MI, Fernandes JV (2002) Surf Coat Technol 149:27
6. Vossen JL, Cuomo JJ (19878) In: Vossen JL, Kern W (eds) Thin film processes, p 15
7. Metals Handbook, 9th Edition, Vol. 2, 1979
8. Beddoes JC, Wallace W, Demalherbe MC (1992) Int J Powder Metal 28(3):313
9. Seetharaman V, Semiatin SL (2002) In: Westbrook JH, Fleischer RL (eds) Intermetallic compounds: vol 3. Principles and Practice, p 653
10. Hashimoto K, Doi H, Tsujimotot T (1986) z. Mat, Trans. JIM 27(2):94
11. Sujata M, Bhargava S, Sangal S (1996) z. ISIJ International 36(3):255
12. Neves F, Marcelo T, Carvalho MH, Trindade B, Vieira MT (2001) Proceedings of EUROMAT 2001, Associazione Italiana di Metallurgia, Milano, 2001
13. Cullity BD (1978) In: Elements of X-Ray Diffraction, Second Edition. Addison-Wesley Publishing Company, Inc., 1978
14. Wegmann G, Gerling R, Schimansky F-P (2003) Acta Mater 51:741
15. Sauthoff G (1995) Intermetallics, VCH FRG, p 14